IRO Journal on Sustainable Wireless Systems (ISSN: 2582-3167)
www.irojournals.com/irosws/

Textile UWB Antennas for Biomedical Applications

S.Bhavani[1*], T. Shanmuganantham[2], N. Mouni[3], G. Jaydeep Sai[4]

[1]Research scholar, Department of electronics engineering, Pondicherry University pondicherry, India
[2]Department of electronics engineering Pondicherry University pondicherry, India
[3,4]Department of ECE, SRGEC, Gudlavalleru, India

E-mail: *ammav10@gmail.com

Abstract

In recent years, there has been an increase in worry about the security of Wireless Body Area Network systems, particularly worn electronics such as military, entertainment, and medical devices. The ability to communicate wirelessly from or to the body via conformal and wearable antennas is a major characteristic of modern wearable electronics. In this work, circular ring and fractal antennas are designed using a wearable substrate of denim with a dielectric constant of 1.7. Design and simulations are carried out in the CST Microwave environment and different performance characteristics of the antenna are examined in free space and on body medical applications.

Keywords: CST, fractal antenna, ring shape, textile substrate, tumor detection.

1. Introduction

The most common imaging methods used to diagnose any organ disorders in the human body are Magnetic Resonance Imaging (MRI), X-ray, Computed Tomography (CT) scan, mammography, and ultrasound scans. However, because of their vast and cumbersome nature, these amenities are not available outside a hospital setting. Furthermore, they are neither fast, inexpensive, transportable, nor are they available in rural health clinics [1, 2]. Recent years have seen the proliferation of Microwave Imaging (MWI) systems for scanning the human body. Points of interest in the system are low in cost, low in complexity, and have a high data flow [3, 24].

Various techniques, such as a slot(s) on the patch and slot(s) implanted on the ground plane, can improve an antenna's efficiency and performance. Patch antennas have recently resurfaced as a fascinating topic in the field of wearable head imaging research. The lower

DOI: https://doi.org/10.36548/jsws.2022.3.004
Received: 07.08.2022, received in revised form: 21.08.2022, accepted: 05.09.2022, published: 15.09.2022

frequency is appropriate for the MWI system [9]. MWI has been recommended as a medical imaging alternative to X-ray, MRI, mammography, and ultrasound for several decades. For these reasons, an effective, simple, non-ionizing, compact, and appealing approach is in high demandas a component of currently applied innovation. For the mostintense radiation-bearing end-fire, the moving wave current stages should be 180 degrees apart on either side. The antenna should have the following characteristics: small size, high data transmission capacity, typically high force rise, directed radiation pattern, and radiation waveform devotion [10]. Separate sorts of antennas for head imaging applications have been developed by researchers based on picture properties for microwaves. Several deserving references including monopoly antenna, directional- Omni directional Ultra-Wide Band (UWB) antenna, Vivaldi antenna, textile antenna and metamaterial antennas etc. were developed [11-28].

2. Materials and Methods

Surprising advancements in the field of MIS have occurred over the years. In medical diagnostic devices, wide frequency band antennas are ideal for obtaining the needed data. An array of antennas, for example, is necessary to progressively obtain a reconstructed picture brain tumor at the L band. In head imaging applications, the small size is important. In general, there are two approaches to building a wideband antenna: using a slot-loaded dipole [4–6] and using a patch or monopole [7].

Li et al., investigated dipole antenna topologies based on Artificial Magnetic Conductor (AMC) reflectors. The authors work using an AMC reflector to shorten the distance between the antenna and the ground plane. For base station applications, Li et al., [5-8] presented a dual-band antenna array. When compared to the Perfect Electrical Conductor (PEC) counterpart, the surface height of the AMC reflector can be cut in half. Li et al., described stacked antenna arrays with a dipole design. The advantage of the stacked structure is that it takes up less room in the aperture.

2.1 Materials

First, textile materials are employed as substrates or conductors in applications for garment integration. Reduced surface wave losses and improved antenna performance are made possible by its low relative permittivity, low loss tangent, and thinner thickness (h). To design and model a microstrip patch antenna, Computer Simulation Technology (CST) microwave studio software is employed. In the design of antennas, copper is utilised for the ground plane and patch. The substrate is essential for antenna design. In order to meet human

needs, wearable antennas must be appropriate for clothes. Different substrates are used to create the antenna in order to determine which is most comfortable to wear. A variety of substrates are used to analyse the antennas at the UWB band, including RT Duroid 5880, GML 1000, RO4003, FR-4, Jeans, Lycra, Rubber, Polyester, Taconic TLC, Bakelite, Arlon AD 250, Wash cotton, Resin, Cordura, Cotton, Quartzel cloth, curtain cotton, and Teflon.

From a design perspective, there are four major stages to divide wearable textile antenna design methodologies. The first stage is to select the material depending on the requirements of the design, which can include substrate and conducting materials. The investigation of the uncharacterized material's electrical properties, such as conductivity, loss tangent, and dielectric constant, must take place in the second phase. The third phase prior to construction involves simulating, optimising, and building wearable textile antennas' radiating elements and feed methods based on the information at hand. The fourth phase involves selecting the fabrication method.

Some of the tests carried out in this work that are not frequently employed in other antenna applications include humidity, temperature, bending impact, and robustness testing. UWB antennas made of fabric, such as cotton and denim, or of plastic as a substrate, can be used as a wearable device on the body because they have no impact on the human body. A paper-based denim material serves as the project's basis. The paper's main contribution is the presenting of a small wearable UWB antenna with line feed and defective ground on a fabric substrate made of denim (r = 1.7). A radiation patch with slots is used in the wearable textile UWB antenna to get the best radiation characteristics in the 3.1 to 10.6 GHz frequency band.

2.2 Design of antenna

The geometries of proposed antennas are shown in fig.1. The parameters of the antenna are optimized. The detailed antenna dimensions are listed in Table 1. The proposed antennas have dimensions of 12mm x 12mm with jeans substrate that has a permittivity of 1.7 and thickness of 1.6 mm. Copper is used for ground as well as for patch with a thickness of 0.035 mm. Line feeding is used with 50ohm matched impedance. The total design done using the dimensions of this antenna have been obtained using CSTMicrowave studio.

Radius of the circular patch controls the mode of the antenna, and the following equation can be used to compute the radius of the circular patch R.

$$R = \frac{F}{\sqrt{\{1+\frac{2h}{\pi Fer}\left[\ln\left(\frac{\pi F}{2h}\right)+1.772\right.}} \quad (1)$$

where F is given by,

$$F = \frac{8.791X10^9}{fr\sqrt{er}} \quad (2)$$

Table 1. Dimensions of the proposed antennas

Parameter	Dimension (mm)
SL(SubstrateLength)	12
SW(SubstrateWidth)	12
h & pt	1.6 & 0.035
FW1,FW2,FW3	5.8, 3.2,2.4
R1,R2,R3,R4	0.3,1.5,3.2,0.9
a, b	0.5,2.5
T1, T2, T3	3.5,2.5,0.5
S1, S2, S3	2,1,0.1
FL1,FL2,FL3	2,4,4

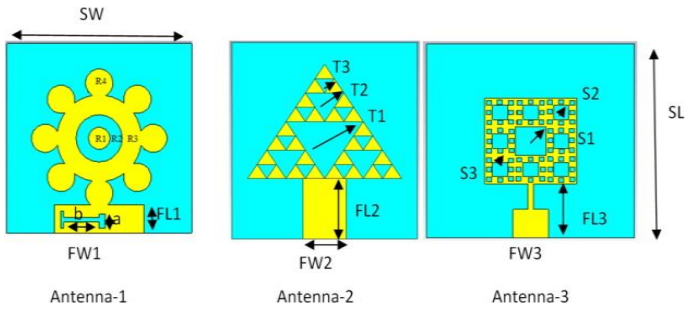

Figure 1. Geometry of the proposed antennas

Substrate's relative permittivity is er, and the height is h. It should be emphasized that the antenna's operational bandwidth must be as big as feasible in order to provide the high resolution to distinguish extremely small tumors. Sierpinski gasket geometry is the most well studied fractal geometry for antenna applications. In this paper's antenna-2 design, Sierpinski gasket geometry is used. A planar triangle is first drawn. The middle triangle is then removed, as shown in the diagram, with its vertices placed at the angles between its sides. The procedure is then carried out once more for the remaining triangles, as seen in figure 2. The Sierpinski gasket fractal is created by endlessly repeating this iterative method. Black triangular patches represent a metallic conductor, while white triangular patches show the area where metals are removed.

Similar to the Sierpinski gasket, the Sierpinski carpet is constructed using squares as opposed to triangles. Starting with a square in the plane, this type of fractal antenna divides it

into nine further smaller congruent squares, dropping the open centre square in the process. Nine smaller, congruent squares are created by dividing the remaining eight squares. Figure 3 illustrates these actions.

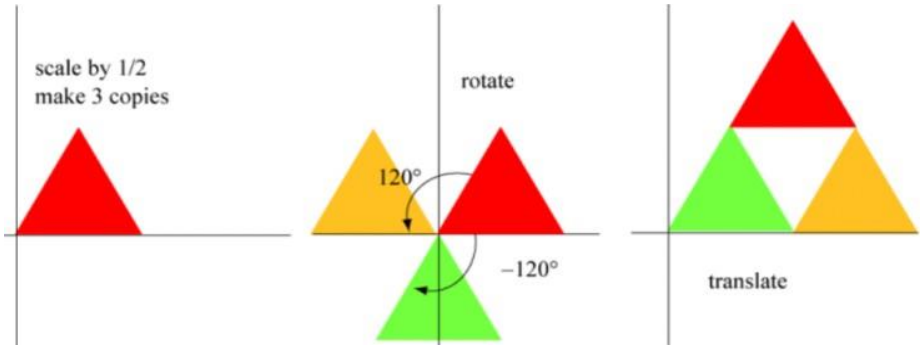

Figure 2. Steps involved in Sierpinski gasket geometry

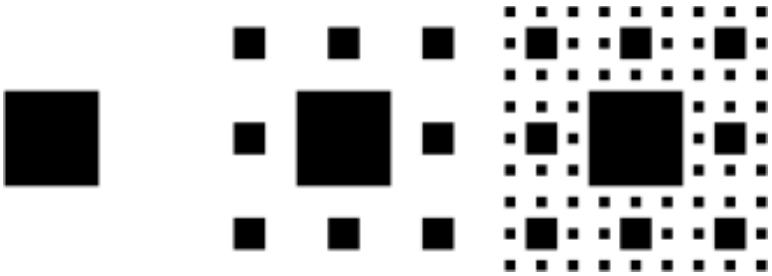

Figure 3. Steps involved in Sierpinski carpet geometry

Table 2. Electrical properties of brain layers

Tissue	Permittivity (F/m)	Electrical Conductance (S/m)
Bone	8.11	2.13
Fat	8.8	1.707
Muscle	42.79	10.62
Skin	31.29	8.01
Thyroid	24.12	12.132
Tumor	4.5	6

3. Phantom Design

3.1 Brain

Using the CST software depicted in Fig. 4, a brain model has been created. For ease of use, a straightforward model is made to look like the human brain. There are six layers,

measuring 35mm, 30mm, 25mm, 20mm, 15mm, and 5mm for the skin, fat, skull, dura, CSF, and brain, respectively. In Table II, three layers' electrical properties are displayed.

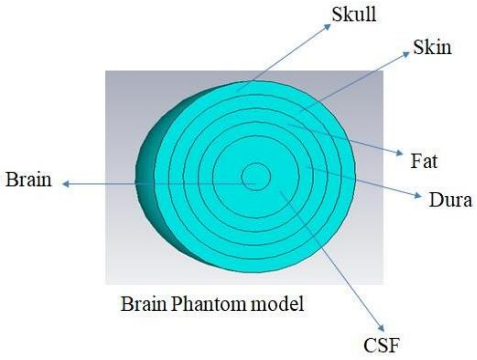

Figure 4. Brain Phantom model

3.2 Thyroid

The CST programme depicted in Fig. 5 is used to create the thyroid model. For ease of use, a straightforward model that closely reflects the human thyroid's anatomy has been created. There are six layers: thyroid, bone, fat, muscle, skin, and tumor [27-28]. Table III displays the electrical properties of six layers.

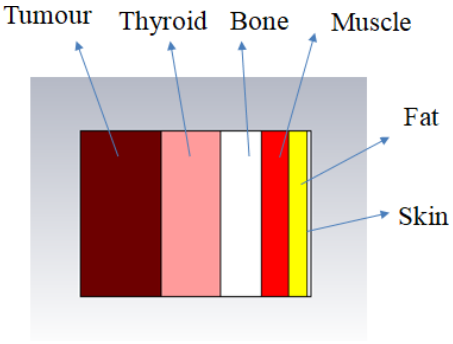

Figure 5. Thyroid model

Table 3. Electrical properties of thyroid layers

Tissue	Permittivity (F/m)	Electrical Conductance (S/m)
Brain	43.22	1.29
CSF	70.1	2.3
Dura	46	0.9
Fat	5.54	0.04
Skin	45	0.73
Skull	5.6	0.03

4. Results & Discussion

Figure 6 depicts an analysis of the antenna's return loss performance. Antenna 1 results in return loss of -44dB with three notches and each notch covers a minimum bandwidth of 500MHz. Due to outer circles of the inner ring, this antenna results in multiple notches. Antenna 2 with triangle shaped slots results in a peak of -40dB at a resonant frequency of 7.8GHz with enhanced bandwidth. Similarly, antenna 3 with square shaped slots results in a return loss of -42dB which covers the complete UWB range.

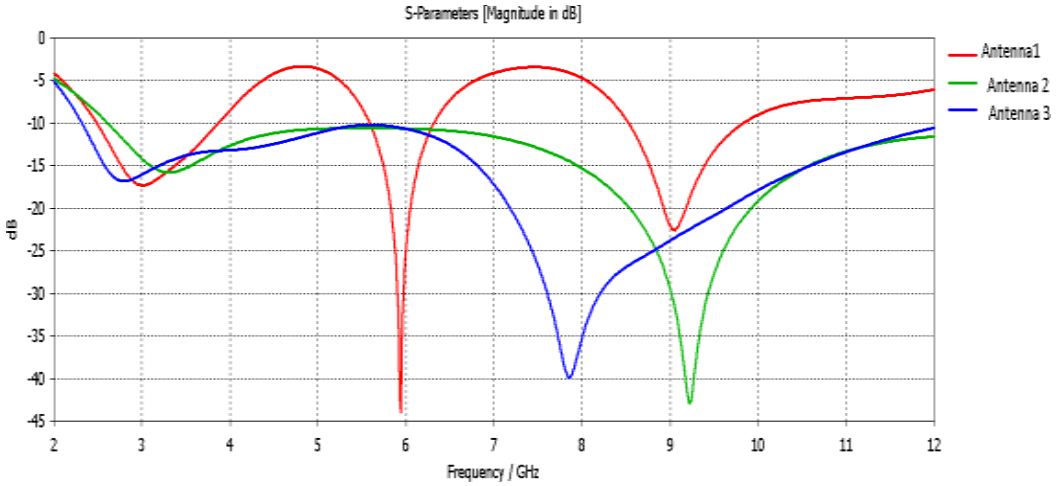

Figure 6. S11 results of antenna models in free space

Proposed antenna is placed in various positions to the brain and thyroid models to get different results. Bending and rotating of antennas are also tested. Introducing the slots in the ground results in a deeper notch.

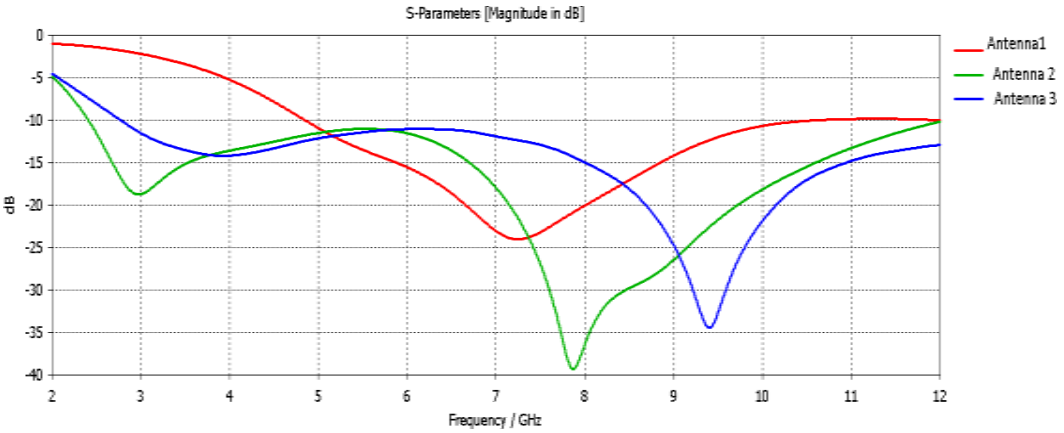

Figure 7. S11 results of antenna models tested on brain model

Designed antennas are placed on the brain model and performance of antennas is tested phantom with and without tumor. The related S11 parameters are presented in figure 7.

Antenna 1 results in a loss of -24dB, antenna 2 results in a peak of -38dB and antenna 3 results in a loss of -34dB. Due to high dielectric properties of the tumor, the S11 values are degraded compared to free space.

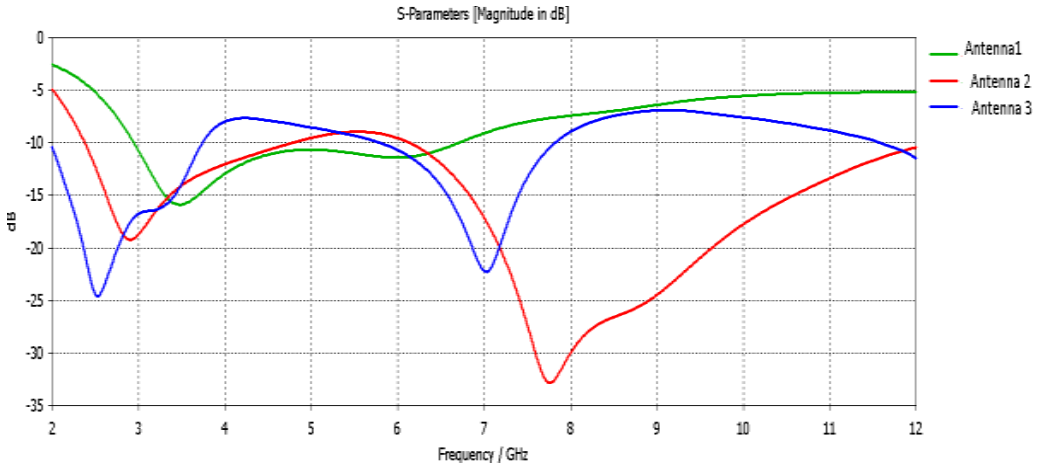

Figure 8. S11 results of antenna models tested on Thyroid model

Designed antennas are tested on the thyroid model and performance of antennas is tested phantom with and without tumor. The related S11 parameters are presented in figure 8. Antenna 1 results in a loss of -16dB, antenna 2 results in a peak of -33dB and antenna 3 results in a loss of -24.8dB. Due to the high dielectric properties of the tumor, the S11 values are degraded compared to free space. Various output parameters for three antennas are compared and tabulated in table 4.

Table 4. Comparison of antennas

Antenna Model	Structure	Resonant frequencies (GHz)	Sll (Peak) (dB)	VSWR	E-Field (V/m)	Directivity (dB)	Gain (dB)	SAR (W/Kg)
1	Designed Antenna (Only Patch)	3,5.98 &9	-44	1.06	20305.6	3.978	2.17	1.13
	Patch with Brain Phantom (Without tumor)	2.9,6.2 &8	-38.5	1.42	277223	3.765	1.92	1.24
	Patch with tumor	7.2	-24	1.75	30980.2	3.038	1.65	1.28
	Patch with Thyroid	3,6&7.5	-25.6	1.56	267875	3.425	1.95	1.36
	Patch with Thyroid tumor	2.9&7.8	-16	1.78	208953	2.986	1.86	1.44
2	Designed Antenna (Only Patch)	3.35&9.2	-43	1.46	213056	4.2	2.5	1.02
	Patch with Brain Phantom (Without tumor)	3.45&9	-42.5	1.6	209223	4.125	2.3	1.43

	Patch with tumor	3&7.9	-39	1.75	209802	3.95	2.25	1.54
	Patch with Thyroid	3.37 &8	-36.2	1.55	20969.5	4.056	2.35	1.28
	Patch with Thyroid tumor	3.4	-32	1.69	203243	3.956	2.22	1.34
3	Designed Antenna (Only Patch)	2.8&7.9	-40	1.23	219652	3.978	2.46	1.22
	Patch with Brain Phantom (Without tumor)	3&8.1	-38.2	1.45	217123	4.026	2.42	1.32
	Patch with tumor	4&9.2	-34	1.54	219802	3.869	2.38	1.48
	Patch with Thyroid	3&7.5	-30.86	1.56	217665	3.98	2.4	1.26
	Patch with Thyroid tumor	2.4&7	-24	1.61	206223	3.6	2.39	1.54

5. Conclusion

The detection of thyroid and brain tumors using a new circular patch antenna has been proposed in this research. Circular patch antennas are compared with triangular and square slotted fractal antennas in implementation. In order to give flexibility for on-body medical applications, these antennas are designed to get around the limitations of the standard methods. A comparison of the results is made between suggested antennas and proposed antennas with brain and thyroid models. Since a wearable application is the primary goal of antenna design, a substrate with a dielectric constant of 1.7 such as a 1.5 mm thick piece of denim has been selected. Using CST Microwave studio, all simulations have been completed.

References

[1] Sohani B, Khalesi B, Ghavami N, et al. Detection of haemorrhagic stroke in simulation and realistic 3-D human head phantom using microwave imaging. Biomed Signal Process Control. 2020;61:102001.

[2] Sohani B, Tiberi G, Ghavami N, Ghavami M, Dudley S, Rahmani A. Microwave imaging for stroke detection: validation on headmimicking phantom. In 2019 Photonics & Electromagnetics Research Symposium-Spring (PIERS-Spring). IEEE; 2019:940-948.

[3] Hasan MM, Samsuzzaman M, Talukder MS, Islam MT, Mahmud MZ, Alam T. Omnidirectional wideband slotted antenna for human head imaging. In 2020 2nd International Conference on Sustainable Technologies for Industry 4.0 (STI). IEEE; 2020:1-4.

[4] Li M, Yasir JM, Zhou C, Jiang L, Yeung KL. A novel dipole configuration with improved out-of-band rejection and its applications in low-profile dual-band dual-polarized stacked antenna arrays. IEEE Trans Antennas Propag. 2020;69:3517-3522.

[5] Li M, Li Q, Wang B, Zhou C, Cheung S. A miniaturized dual-band base station array antenna using band notch dipole antenna elements and AMC reflectors. IEEE Trans Antennas Propag. 2018;66(6):3189- 3194.

[6] Li M, Li Q, Wang B, Zhou C, Cheung S. A low-profile dual-polarized dipole antenna using wideband AMC reflector. IEEE Trans Antennas Propag. 2018;66(5):2610-2615.

[7] Talukder MS, Samsuzzaman M, Hasan MM, Islam MT, Hossain I, Singh MSJ. Chinese temple shaped slotted monopole UWB patch antenna for microwave imaging applications. In 2021 International Conference on Information and Communication Technology for Sustainable Development (ICICT4SD). IEEE; 2021:249-253.

[8] Li M, Wang R, Yasir JM, Jiang L. A miniaturized dual-band dual- polarized band-notched slot antenna array with high isolation for base station applications. IEEE Trans Antennas Propag. 2019;68(2):795- 804.

[9] Salleha CCYA, Alama T, Singha MSJ, Samsuzzamanc M, Islama MT. Development of microwave brain stroke imaging system using multiple antipodal. J Kejuruterran. 2020;32:1-6.

[10] Wu B, Ji Y, Fang G. Design and measurement of compact tapered slot antenna for UWB microwave imaging radar. In 2009 9th International Conference on Electronic Measurement & Instruments. IEEE; 2009:2- 226-2-229.

[11] Ojaroudi M, Bila S, Salimi M. A novel approach of brain tumor detection using miniaturized high-fidelity UWB slot antenna array. In 2019 13th European Conference on Antennas and Propagation (EuCAP). IEEE; 2019:1-5.

[12] Inum R, Rana M, Shushama KN, Quader M. EBG based microstrip patch antenna for brain tumor detection via scattering parameters in microwave imaging system. Int J Biomed Imaging. 2018;2018:8241438.

[13] Borja B, Tirado JA, Jardon H. An overview of UWB antennas for microwave imaging systems for cancer detection purposes. Prog Electromagn Res B. 2018;80:173-198.

[14] Islam M, Mahmud M, Islam MT, Kibria S, Samsuzzaman M. A low cost and portable microwave imaging system for breast tumor detection using UWB directional antenna array. Sci Rep. 2019;9(1):1-13.

[15] Jamlos M, Jamlos M, Ismail A. High performance novel UWB array antenna for brain tumor detection via scattering parameters in microwave imaging simulation system, in

2015 9th European Conference on Antennas and Propagation (EuCAP). IEEE; 2015:1-5.

[16] Ullah S, Ruan C, Sadiq MS, Haq TU, He W. High efficient and ultra wide band monopole antenna for microwave imaging and communication applications. Sensors. 2020;20(1):115.

[17] Salleh A, Yang CC, Singh MSJ, Islam MT. Development of antipodal Vivaldi antenna for microwave brain stroke imaging system. Int JEng Technol. 2019;8(3):162-168.

[18] Mobashsher AT, Abbosh AM. Compact 3-D slot-loaded folded dipole antenna with unidirectional radiation and low impulse distortion for head imaging applications. IEEE Trans Antennas Propag. July 2016;64(7):3245-3250.

[19] Rokunuzzaman M, Ahmed A, Baum TC, Rowe WS. Compact 3-D antenna for medical diagnosis of the human head. IEEE Trans Antennas Propag. 2019;67(8):5093-5103.

[20] Alqadami AS, Bialkowski KS, Mobashsher AT, Abbosh AM. Wearable electromagnetic head imaging system using flexible wideband antenna array based on polymer technology for brain stroke diagnosis. IEEE Trans Biomed Circuits Syst. 2018;13(1):124-134.

[21] Alqadami AS, Nguyen-Trong N, Mohammed B, Stancombe AE, Heitzmann MT, Abbosh A. Compact unidirectional conformal antenna based on flexible high-permittivity custom-made substrate for wearable wideband electromagnetic head imaging system. IEEE Transactions on Antennas Propag. 2019;68(1):183-194.

[22] Talukder MS, Samsuzzaman M, Hasan MM, Islam MT, Islam MT, Rahman MN. Square enclosed circle microstrip patch antenna for microwave head imaging. In 2020 23rd International Conference on Computer and Information Technology (ICCIT). IEEE; 2020:1-5.

[23] Yin B, Ye M, Yu Y. A novel compact wearable antenna design for ISM band. Prog Electromagn Res C. 2021;107:97-111.

[24] Yahya R, Kamarudin MR, Seman N. New wideband textile antenna for SAR investigation in head microwave imaging. In 2014 IEEE MTT-S International Microwave Workshop Series on RF and Wireless Technologies for Biomedical and Healthcare Applications (IMWS- Bio2014). IEEE; 2014:1-3.

[25] Hossain A, Islam MT, Chowdhury ME, Samsuzzaman M. A grounded coplanar waveguide-based slotted inverted delta-shaped wideband antenna for microwave head imaging. IEEE Access. 2020;8:185698- 185724.

[26] Islam MS, Islam MT, Hoque A, Islam MT, Amin N, Chowdhury ME. A portable electromagnetic head imaging system using metamaterial loaded compact directional 3D antenna. IEEE Access. 2021;9:50893- 50906.

[27] J. Jenisha and K. Madhan Kumar, Design Of H-Shape Microstrip Patch Antenna For Wearable Applications To Detect The Thyroid Gland Cancer Cells, Ictact Journal On Microelectronics, JULY 2020, VOLUME: 06, ISSUE: 02.

[28] I. Sheeba, Study on the Design and Implementation of Flexible Wearable Antenna on Thyroid Gland in the Detection of Cancer Cells, 21 July 2021, Current Approaches in Science and Technology Research Vol. 12.